Eurographics Symposium on Rendering (2022)
A. Ghosh and L.-Y. Wei (Guest Editors)

Polarization-imaging Surface Reflectometry using Near-field Display

E. Nogué[1,2], Y. Lin[2], A. Ghosh[1,2]

[1]Imperial College London
[2]Lumirithmic Ltd

(a) Photo (b) Diff. (c) Spec. (4×) (d) Roughness (e) Normals (f) Rendering 1 (g) Rendering 2

Figure 1: A planar sample (notebook cover) (a) imaged at near-Brewster angle lit by a near-field display (iPad Pro). Polarization-imaging of sample in conjunction with controlled display illumination enables estimation of high-quality SVBRDF maps (b – e). Rendering of sample with point light from front (f), and 45° from above (g).

Abstract

We present a practical method for measurement of spatially varying isotropic surface reflectance of planar samples using a combination of single-view polarization imaging and near-field display illumination. Unlike previous works that have required multiview imaging or more complex polarization measurements, our method requires only three linear polarizer measurements from a single viewpoint for estimating diffuse and specular albedo and spatially varying specular roughness. We obtain high-quality estimate of the surface normal with two additional polarized measurements under a gradient illumination pattern. Our approach enables high-quality renderings of planar surfaces while reducing measurements to a near-optimal number for the estimated SVBRDF parameters.

CCS Concepts

• ***Computing methodologies*** → ***Rendering; Image and video acquisition;***

1. Introduction

Appearance modeling of real-world surfaces has been an active area of research in graphics and vision with a wide range of applications including entertainment, AR/VR, cultural heritage, advertising, product design etc. Advances in digital imaging has resulted in image based measurements becoming an integral component of appearance modeling. A recent trend here has been towards more practical acquisition techniques, employing commodity off-the-shelf equipment.

In this work, we aim to further simplify surface reflectometry with minimal measurements using commodity equipment. Similar to prior works in computer graphics, we exploit polarization imaging [RRFG17], as well as controlled display illumination [GCP*09, FCMB09, AWL13] for this purpose. However, we exploit novel cues in polarized surface reflectance to reduce measurements compared to prior work for estimating a complete set of reflectance maps for spatially varying planar surfaces exhibiting isotropic reflectance. Our method and analysis is strictly valid only for dielectric surfaces. We also obtain partial results for samples with some metallic surface patches by employing a heuristics based processing of the measurements.

Our simple capture setup involves a camera with a linear polarizer observing a planar sample at an oblique (near Brewster) orientation while the sample is lit by near-field illumination from a display (Fig. 1, a). We demonstrate how just three measurements of the surface with different orientations of the linear polarizer under a fixed display illumination is sufficient to obtain high-fidelty estimates of diffuse and specular albedo, and spatially varying specular roughness, as well as providing partial cue for surface normals. Two additional polarization measurements under another gradient illumination pattern emitted by the display enables complete estimate of the surface normals. Thus, *just five* measurements are required with our method from a fixed viewpoint using a standard DSLR camera with a rotating linear polarizer to estimate the entire set of spatially varying BRDF parameters (Fig. 1, b – e), which is

near optimal in terms of the number of estimated parameters! Given the recent availability of polarization sensing cameras, the method reduces to *just two* measurements with such specialized polarization sensors.

In summary, the principal contributions of this work are:

- A practical method for acquisition of spatially varying surface reflectance of planar samples with reduced measurements using commodity components.
- Improved estimates of diffuse and specular albedo, and novel estimation of spatially varying specular roughness from polarization imaging of reflectance under a single lighting condition.
- Novel estimate of surface normals requiring two additional polarization measurements under a second (gradient) illumination condition.

2. Related Work

We will limit the discussion in this section to the most relevant previous works. For a more detailed review on appearance capture and modeling, we direct the interested reader to existing surveys on the topic [WLL*09, GGG*16].

2.1. Extended Illumination

Extended illumination sources have been preferred over point sources for SVBRDF measurement of planar surfaces. Gardner et al. [GTHD03] employed a linear light source mounted on a translation gantry in order to record per-pixel reflectance traces of planar samples. This design was later modified by Ren et al. [RWS*11] for portability, and Chen et al. [CDP*14] to allow measurement of anisotropic BRDFs. Extended area sources such as display panels have been employed as an alternative to linear light sources to help further reduce the amount of data and time spent in measurements. For homogeneous samples, Wang et al. [WSM11] have proposed employing step edge illumination for a dual-scale statistical modeling of surface appearance. Close to our approach, Ghosh et al. [GCP*09] proposed to emit second order gradient illumination patterns from an LCD screen to estimate spatially varying reflectance maps of planar samples, and exploited the inherent polarization of LCD illumination for diffuse-specular separation. This approach was also adopted by Riviere et al. [RPG16] for a tablet-based capture. Francken et al. [FCMB09] instead proposed employing Gray codes for this purpose, while Aittala et al. [AWL13] have proposed to capture a sample's response to band-limited illumination patterns in the frequency domain using 2D Fourier patterns. While we employ a near-field display similar to Aittala et al., our method requires a significantly reduced number of measurements compared to these above methods for SVBRDF measurement of planar samples.

2.2. Exploiting polarization

Researchers have extensively looked at polarization imaging, both exclusively [WB91, Mül95, DHT*00, MHP*07], as well as in conjunction with color space methods [NFB97], for diffuse-specular separation. These methods all exploit the fact that diffuse reflection tends to depolarize incident polarized illumination due to multiple subsurface scattering, while specular reflection preserves incident polarization due to single bounce. Ma et al. [MHP*07] proposed combining polarization with spherical gradient illumination (using an LED sphere) to obtain high quality diffuse and specular albedo and normal maps. Their view dependent polarization solution was later extended for multi-view capture [GFT*11]. Close to our work, Ghosh et al. [GCP*10] have proposed measurement of the complete Stokes parameters of reflected circularly polarized uniform illumination to recover detailed reflectance parameters including index of refraction and specular roughness. We demonstrate these appearance parameters can be estimated from just the three linear polarizer measurements for planar samples without requiring a circular polarizer measurement. Also related is the work of Miyazaki et al. [MTHI03], who employ linear polarization imaging under unpolarized illumination coupled with inverse rendering in order to estimate shape, albedo and specular roughness of a homogeneous convex object. Our work is closest to and builds upon that of Riviere et al. [RRFG17] who employ similar near-Brewster angle polarization imaging for surface reflectometry in uncontrolled outdoor environments. They however require multiview imaging for surface normals and a light probe measurement for inverse rendering to estimate specular roughness. We instead show how controlled near-field display illumination simplifies SVBRDF measurements of planar samples. Toisoul et al. [TDG18] have also employed similar polarization measurements for printed holographic samples. However, they focus on estimating spatially varying diffraction grating orientation instead of SVBRDFs.

Shape from polarization has been previously studied in the vision literature, with the angle of polarization determining the direction perpendicular to the plane of incidence. This is usually combined with the degree of polarization which reaches an extremum at Brewster angle for specular polarization [TVC07, SSIK99]. Shape from polarization has also been studied for diffuse polarization [AH06]. We account for both types of polarization to obtain partial information of the surface normal from our measurements.

Recent work of Baek et al. has extensively studied polarization characteristics of surface reflectance through complete Mueller matrix measurements, coupled with inverse rendering using a pBRDF model that includes diffuse and specular polarization in order to estimate spatially varying BRDFs of objects [BJTK18] and dense pBRDF measurements of homogenous material samples [BZK*20]. These methods are very powerful in the range of material appearance parameters that can be inferred but require rather complex measurement setups and significantly large number of measurements. Instead, we show SVBRDFs of planar samples can be resolved with a much simpler polarization measurement process. Polarization cues have also been exploited recently in conjunction with deep learning to estimate surface normals [BGW*20] and full SVBRDF parameters of 3D objects [DLG21]. Our method directly estimates all SVBRDF parameters without requiring any deep learning while keeping the number of required measurements to a minimum.

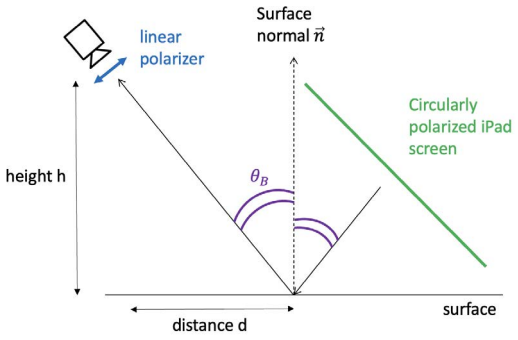

Figure 2: Measurement setup diagram.

(a) IH (b) IV

Figure 3: Colorchart and a black plastic comb employed as reference calibration objects for diffuse and speclar reflectance respectively. We note diffuse polarization effects on the diffuse squares of the colorchart where the IV measurement is brighter than IH.

3. Method

3.1. Measurement Setup

Our proposed setup for SVBRDF measurement of planar isotropic samples consists of a tripod mounted DSLR camera (Canon 850D) with a lens-mounted linear polarizer observing the sample from a distance $d = 1.0m$ at near Brewster angle of incidence. Here, we define the Brewster angle as that of an average dielectric material with refractive index $\eta = 1.45$ such that the camera view vector forms an incident angle equal to Brewster angle $\theta_B = \arctan(1.45)$ with the up vector $(0,0,1)$. The sample is illuminated with a near-field display, an iPad Pro tablet screen in our case, from the mirror reflection direction with respect to the camera view (see Fig. 2). We prefer the display to be near-field instead of far-field in order to cover a larger sample with direct illumination from a tablet and also to have brighter illumination on the sample. We employ auto-exposure-bracketing on the camera for HDR imaging for higher quality measurements, and manually rotate the polarizer on the camera for polarization imaging of the observed surface reflectance.

We assume the illumination from the display to be unpolarized and exploit the polarization property of Brewster angle reflection for surface relectance analysis similar to the approach of [RRFG17]. We note that the screen of the iPad Pro tablet we employ is circularly polarized. However, for linear polarization measurements of reflectance on a dielectric surface, this is equivalent to unpolarized illumination. At near Brewster angle of incidence,the Fresnel reflectivity coefficient $R_{||}$ for a dielectric should be close to zero. Similarly to unpolarized illumination, this renders circularly polarized illumination to reflect as completely linearly polarized ($R_{\perp}$) at Brewster angle [GCP*10], and this a property that we exploit for reflectance analysis in our setup.

3.2. Specular and Diffuse Albedo

We illuminate the sample with a specific illumination pattern from the screen designed for uniform specular reflectance over the sample surface. We compute this pattern, which we refer to as the albedo pattern, using simulation of the near-field illumination from the screen on a smooth planar dielectric surface using Mitsuba 2 [NDVZJ19]. The albedo pattern creates a slight vertical gradient of intensity (with a low slope) across the screen which results in relatively even specular reflectance over a fixed area of measurement.

We carry out three linear polarization measurements of surface reflectance under the albedo illumination pattern with the polarizer oriented at 0°, 45°, and 90° respectively. We refer to these images in the following as IH, I45 and IV respectively.

For specular and diffuse separation and albedo estimation, we need to consider only the IH and IV images. Since specular reflectance at near Brewster angle is completely $\perp$ polarized, IV is almost completely diffuse. On the other hand, IH contains strong specular signal of the $R_{\perp}$ specular component. Riviere et al. [RRFG17] have previously proposed polarization difference imaging (IH - IV) to isolate the $R_{\perp}$ specular component under the assumption of equal amounts of mostly unpolarized diffuse reflectance in both IH and IV. While this assumption may hold for the case of hemispherical environmental illumination in outdoor environments, in our case we have a strong directional illumination from the tablet display. We observe measureable diffuse polarization effects in surface reflectance with our setup, which is consistent with previous studies on diffuse polarization [AH06]. This results in diffuse reflectance being brighter in the IV image (maxima of diffuse polarization) and darker in the IH image (minima of diffuse polarization). We measured this diffuse polarization effect due to the screen illumination on the diffuse white/gray squares of a color checker chart and found the diffuse intensity reduces by up to 12% in IH compared to IV, and that the reduction in intensity follows a sinusoid with rotation angle of the polarizer (see Fig. 3). Thus, isolation of $R_{\perp}$ specular component cannot be obtained from a simple difference imaging but requires a scaled difference:

$$R_{\perp} = IH - IV * \gamma, \tag{1}$$

where the diffuse scaling γ varies along a sinusoid from 1.0 to 0.88 with polarizer orientation at 90° (IV) to 0° (IH). Accounting for diffuse polarization variation in the polarization difference imaging allows us to isolate the $R_{\perp}$ specular reflectance more ac-

(a) Uneven diffuse in IV (b) Even diffuse albedo

Figure 4: Measured uneven diffuse in IV (a), and normalized diffuse albedo (b).

curately which improves subsequent estimation of refractive index η described next.

3.2.1. Specular calibration

Given the estimated $R_\perp$, we follow [RRFG17] to estimate the refractive index η from the Brewster angle measurement as $\eta = \sqrt{\frac{1+\sqrt{R_\perp{}'}}{1-\sqrt{R_\perp{}'}}}$. Here $R_\perp{}'$ is the scaled Brewster angle specular reflectance where the scaling factor is obtained using a calibration target. We employ a smooth black plastic surface (a black plastic comb) with a known refractive index of $\eta_{plastic} = 1.45$ for this specular reflectance calibration. Finally, we obtain R_0 the Fresnel specular reflectance at normal incidence from η as:

$$R_0 = (\frac{1-\eta}{1+\eta})^2. \tag{2}$$

R_0 is the estimated specular albedo ρ_s for rendering.

3.2.2. Diffuse calibration

Similar to the specular reflectance calibration, we also need to calibrate the diffuse reflectance observed in IV. We employ an IV measurement of the white/gray squares on a color checker chart for this absolute diffuse reflectance calibration. However, despite this global intensity scaling wrt color chart, the calibrated diffuse measurement IV is not the diffuse albedo. This is because the measurement is under the specular albedo illumination pattern which, while creating a uniform specular reflectance over the sample, creates an uneven diffuse reflectance over the sample surface (see Fig. 4, a). We normalize this uneven brightness of diffuse reflectance over the sample surface using a pre-computed lookup table of diffuse brightness variation over a spatial extent due to our near-field display illumination. We pre-compute this lookup table using simulation in Mitsuba 2. Fig. 4 (b) shows the diffuse intensity after lookup table based normalization which can be employed as the diffuse albedo ρ_d for rendering.

3.3. Specular Roughness from Polarization

One of the principal contributions of our work is the estimation of spatially varying specular roughness from polarization measurements. We employ Cook-Torrance BRDF model in our work and

(a) $R_\perp$ (b) R0 (c) Power func.

Figure 5: Measured $R_\perp$ (a), estimated R_0 (b), and a power visualization function of their ratio providing cue for specular roughness (c).

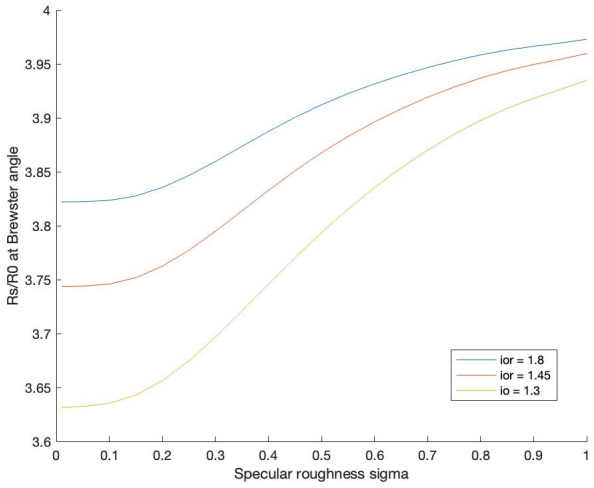

Figure 6: $R_\perp/R_0$ variation due to increasing specular roughness σ at various refractive indices $\eta \in [1.3, 1.45, 1.8]$.

define specular roughness σ in terms of the slope of the microfacets of the Beckmann distribution.

Given the measurement of perpendicular polarized specular reflectance at Brewster angle $R_\perp$, and the corresponding estimate of reflectance at normal incidence R_0 via the estimate of refractive index η (Eq.2), we make the novel observation that the ratio $R_\perp/R_0$ provides a cue for specular roughness. Fig. 5 (c) shows a power visualization function employed to increase contrast and give a better visualization of $R_\perp/R_0$ to illustrate its relation to specular roughness variation on the sample. The power function is $f(\mathrm{R}_\perp/R_0)=(\mathrm{R}_\perp/R_0/C))^8$ where $C = 4.5$ is a maximal value seen in $R_\perp/R_0$ ratio. In order to extract specular roughness values from the ratio, we build a pre-computed look-up table using simulations in Mitsuba 2. Our simulations indicate that for a fixed index of refraction η, the ratio $R_\perp/R_0$ increases monotonically with specular roughness, as seen in Fig. 6. For a planar dielectric sample, each imaged surface point can be independently analysed using the polarization measurements to estimate the spatially varying index of refraction and compute the spatially varying ratio $R_\perp/R_0$, which then provides an estimate of specular roughness value via this lookup table.

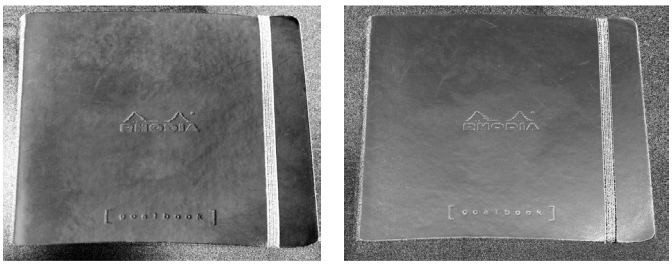

(a) AoLP (3×) (b) Y-gradient ratio

Figure 7: Angle of Linear Polarization (AoLP) (a), and specular ratio of Y-gradient to uniform illumination (b) providing cues for the surface normal.

3.4. Surface Normal exploiting Polarization

Similar to previous work on Shape-from-Polarization, we also exploit the three linear polarizer measurements IH, I45 and IV to obtain cues for the surface normal map. It is well known that the angle of linear polarization (AoLP) fixes the plane of polarization containing the surface normal and for an upwards facing planar surface like in our setup, this also removes the Π-ambiguity of AoLP. Previous works have either employed multiview imaging for uniquely determining the normal in the plane of incidence [RRFG17], or tried to estimate it from the degree of polarization cue [TVC07, SSIK99]. We found the degree of polarization to not be a reliable cue in our setup due to it being affected by both specular and diffuse polarization. Furthermore, we did not measure much variation in the degree of polarization on planar samples in order to exploit it as a cue for surface normal.

Hence, we take a practical approach of determining one degree of freedom of the normal (in spherical coordinates) from the AoLP, while explicitly doing another measurement under a gradient illumination condition emitted by the tablet display in order to determine the second degree of freedom of the normal. For each point on our sample we retrieve two angles α and β illustrated in Fig. 8 which determine the surface normal in spherical coordinates. We can compute the AoLP shown in Fig. 7 as $\chi = 0.5 * \arctan(s2/s1)$, where $s1$ and $s2$ are the linear Stokes parameters that can be determined from our three linear polarization measurements under the uniform specular albedo lighting condition. This angle also known as the ellipticity angle of the polarization ellipse, yields the rotation of the plane of incidence around the view vector $\vec{v}$. Because our surface might naturally have a slight orientation we center the AoLP values on 0. This shift yields a beta angle varying from $-\pi/2$ to $\pi/2$, the first part of our normal map computation.

We obtain the alpha angle through a ratio of specular measurements under a vertical gradient illumination condition and the uniform specular albedo illumination condition. Note that the specular albedo condition is not completely constant and has a small slope to account for the near-field effects. We further modulate this albedo condition with a vertical linear gradient to create the gradient illumination and record the specular response using polarization difference imaging. The ratio of specular intensity on our sample under the $\vec{y}$ gradient illumination and the uniform albedo illumination

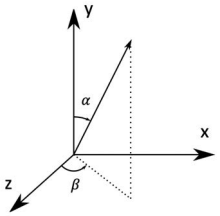

Figure 8: Normal map coordinate system with α the vertical (in-plane) normal variation and β the inclination of the plane of incidence.

yields a measure of the surface orientation in the $\vec{y}$ direction (actually the reflection vector), as seen in Fig. 7 (b). We apply f : x $\mapsto$ 1 - x to this ratio data and then shift the values to $[\frac{-\pi}{2}; \frac{\pi}{2}]$ space, to obtain our α angle. The last step is conversion from the spherical coordinates (α, β) to Cartesian coordinates which provides the specular reflection vector $\vec{r}$. Finally, the surface normal $\vec{n}$ can be obtained as the half-vector between $\vec{r}$ and the view-vector $\vec{v}$ (see Fig. 1, e).

4. Results

Fig. 16 presents additional examples of SVBRDF maps estimated for planar samples using our proposed method, similar to the example shown in Fig. 1. The method is able to estimate high quality maps for materials with dark albedo and significant surface mesostructure variation.

Figs. 9 and 10 present qualitative comparisons of SVBRDF maps for two different planar samples measured by our method vs. those measured using polarized second order gradient illumination emitted by a desktop LCD panel [GCP*09]. As can be seen, the maps measured by our proposed method are qualitatively quite comparable, and even superior in the case of estimation of specular albedo and spatially varying specular roughness, while requiring only half the number of measurements (5 photographs in our case vs 10 photographs for [GCP*09]). We note that the diffuse albedo estimated by our method is slightly brighter due to diffuse polarization in the IV measurement, while our specular albedo is slightly darker than that of [GCP*09] and colorless. This is because the measurement method of [GCP*09] includes some polarization preserving single scattering in the specular albedo. This is why our specular albedo and roughness maps have more contrast as they do not have any residual single scattering.

Figs. 11 and 12 present qualitative comparisons of SVBRDF maps for two different planar samples measured by our method vs. SVBRDF maps recovered by the neural network of [DAD*18] from a single flash-lit image. Although the maps extracted by the network (bottom row) present very consistent maps with continuous normal map variation, they retain artifacts due to the flash illumination and are very limited in resolution.

We render in Fig. 13 SVBRDF maps obtained by our method, under an area light source in Mitsuba 2. The scene configuration is identical to the real-life measurement setup. We compare these renderings to photographs of the samples lit by a uniform tablet

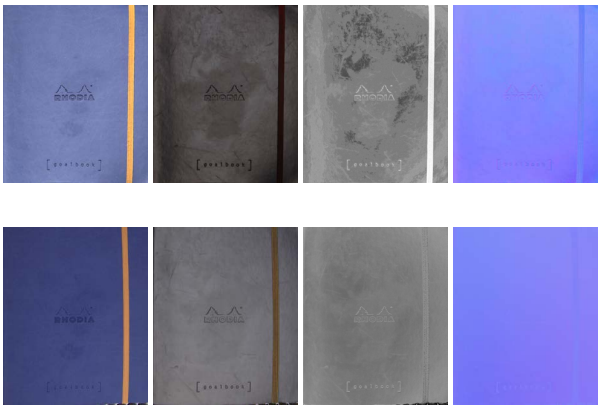

Figure 9: Comparison of estimated SVBRDF maps using our method (top row) vs. [GCP*09] (bottom row)

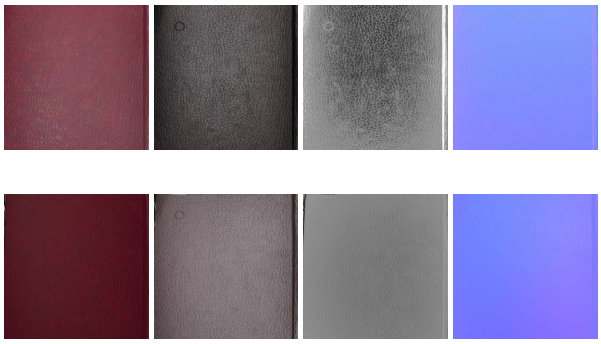

Figure 10: Comparison of estimated SVBRDF maps using our method (top row) vs. [GCP*09] (bottom row)

screen illumination. It is noticeable that on larger samples, such as the red book on the second row, incident angles grow further away from Brewster angle on the sample's edges. This leads to a more difficult separation of diffuse and specular, and therefore a larger error margin in the estimation of roughness and normal maps. The observable consequence is blurry specular reflections on the edges of the larger sample.

4.1. Metallic Surfaces

Fig. 14 and 15 presents partial failure cases for our method of two samples with significant metallic surface patches – a greeting card and a book cover. Here, we note that the metallic surface patches elliptically polarize incident circularly polarized light from the tablet screen. We cannot measure this ellipticity with our measurements since we only employ a linear polarizer on the camera. However, we do observe that the IV measurement is brighter than the IH measurement for the metallic surfaces which is the opposite behaviour compared to dielectric surfaces. We employ this as a cue to classify surface points on the sample as metallic vs dielectric and for metallic surface points, attribute the surface reflectance to the specular albedo. However, due to partial polarization measurement, we

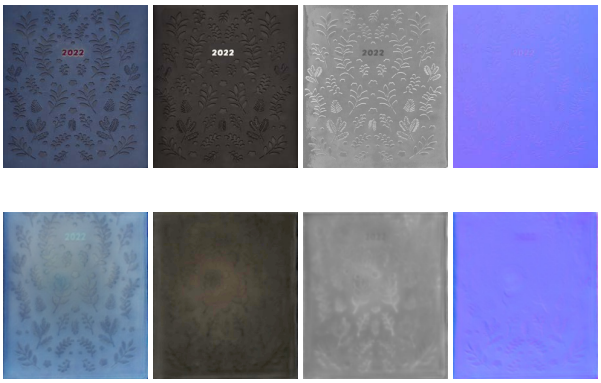

Figure 11: Comparison of estimated SVBRDF maps using our method (top row) vs. [DAD*18](bottom row)

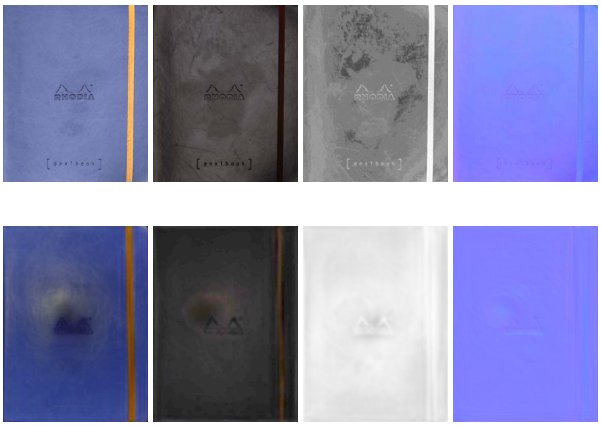

Figure 12: Comparison of estimated SVBRDF maps using our method (top row) vs. [DAD*18](bottom row)

cannot correctly recover the phase and angle of polarization which affects surface normal estimation. We also do not estimate specular roughness for the metallic surface patches and instead set the roughness to a constant value of 0.1.

5. Limitations

Our method has a number of limitations. Due to limited spatial extent of the near-field display, our setup can only illuminate planar samples of a limited size and larger samples can have inaccurate measurements towards the sides and edges which do not receive direct illumination from the display. The sample size is also limited by the assumption of near-Brewster angle measurement. Even if a very large display is employed, for a much larger sample some parts of the sample would be measured away from the Brewster angle, compromising the quality of diffuse-specular separation and subsequent reflectance analysis. Our method is also designed for isotropic dielectric samples. While we show some examples with metallic surface patches, the method does not work accurately on metals. This is because metals elliptically polarize reflected illumi-

Figure 13: Comparison of photographs (left) to Mitsuba2 renderings (right) created using the SVBRDF maps estimated by our method

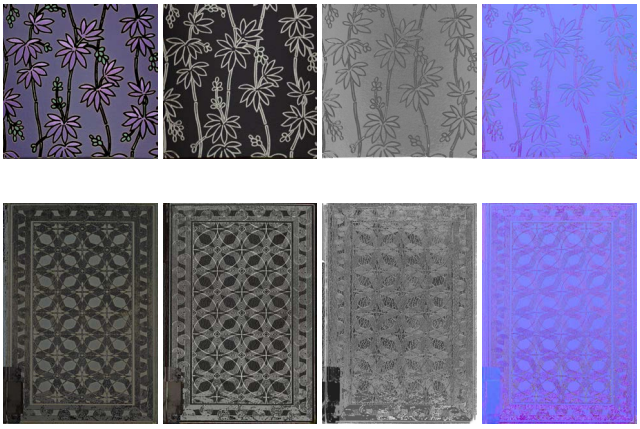

(a) Diff. (b) Spec. (4×) (c) Roughness (d) Normals

Figure 14: Examples of metallic samples measured by our method. Our method estimates specular albedo for the metallic patches but does not provide accurate measurements of the surface normal or specular roughness.

nation which our setup does not account for through the measurements and this affects the surface normal estimate due to ellipticity effecting the AoLP. We currently only estimate the specular albedo of such metallic patches, while setting specular roughness to a constant value. Finally, even for dielectric samples, due to the oblique view on the sample at near-Brewster angle, we do not obtain a good view of some top edges of the sample due to view foreshortening which affects the SVBRDF maps we estimate.

6. Conclusion

We have presented a practical method for surface refectometry of planar SVBRDF samples exhibiting isotropic dielectric reflectance which significantly reduces the number of measurements. We

(a) Rendering1 (b) Rendering2

Figure 15: Renderings of metallic samples in Fig. 15 under a point light source from front (a), and from 45° above (b).

demonstrate how combination of single-view polarization imaging in conjunction with controlled illumination from a near-field display can enable estimation of complete set of SVBRDF parameters using just five measurements which is near optimal for the parameters (five unknowns). Our method can be further reduced to a two-shot capture process using polarization-sensing cameras that are now commercially available. Furthermore, we demonstrate how just three linear polarizer measurements under a fixed display illumination can provide high-quality estimates of diffuse and specular albedo and spatially varying specular roughness, as well as partial information about the surface normal. Future work can focus on more accurately resolving metallic reflectance on material samples as well as extending such a reflectometry approach to anisotropic samples.

Acknowledgments

We thank the reviewers for their extensive feedback. This project has received funding from the European Union's Horizon 2020 research and innovation programme under the Marie Skłodowska-Curie grant agreement No 956585.

References

[AH06] ATKINSON G., HANCOCK E. R.: Recovery of surface orientation from diffuse polarization. *Image Processing, IEEE Transactions on 15*, 6 (2006), 1653–1664. 2, 3

[AWL13] AITTALA M., WEYRICH T., LEHTINEN J.: Practical SVBRDF capture in the frequency domain. *ACM Trans. on Graphics (Proc. SIGGRAPH) 32*, 4 (2013). 1, 2

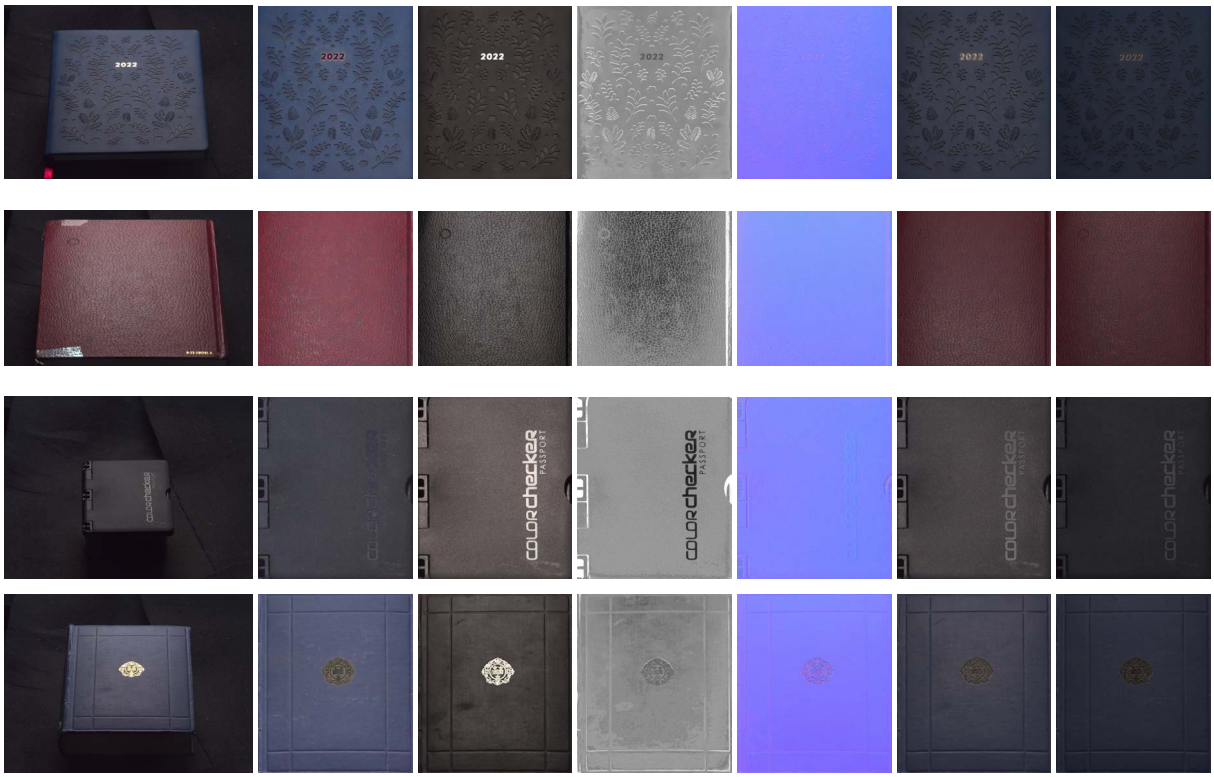

(a) Photo (b) Diff. (c) Spec. (4×) (d) Roughness (e) Normals (f) Rendering1 (g) Rendering2

Figure 16: Additional examples of planar samples measured by our method. High-quality SVBRDF maps (b – e) estimated using single-view polarization imaging at near-Brewster angle (a). Rendering with a point light source from front (f), and from 45° above (g).

[BGW*20] BA Y., GILBERT A., WANG F., YANG J., CHEN R., WANG Y., YAN L., SHI B., KADAMBI A.: Deep Shape from Polarization. In *Lecture Notes in Computer Science (including subseries Lecture Notes in Artificial Intelligence and Lecture Notes in Bioinformatics)* (2020), vol. 12369 LNCS, Springer Science and Business Media Deutschland GmbH, pp. 554–571. 2

[BJTK18] BAEK S.-H., JEON D. S., TONG X., KIM M. H.: Simultaneous acquisition of polarimetric svbrdf and normals. *ACM Trans. Graph. 37*, 6 (dec 2018). 2

[BZK*20] BAEK S. H., ZELTNER T., KU H. J., HWANG I., TONG X., JAKOB W., KIM M. H.: Image-based acquisition and modeling of polarimetric reflectance. *ACM Transactions on Graphics 39*, 4 (2020). 2

[CDP*14] CHEN G., DONG Y., PEERS P., ZHANG J., TONG X.: Reflectance scanning: Estimating shading frame and brdf with generalized linear light sources. *ACM Trans. Graph. 33*, 4 (July 2014), 117:1–117:11. 2

[DAD*18] DESCHAINTRE V., AITTALA M., DURAND F., DRETTAKIS G., BOUSSEAU A.: Single-image SVBRDF capture with a rendering-aware deep network. *ACM Transactions on Graphics 37*, 4 (2018). 5, 6

[DHT*00] DEBEVEC P., HAWKINS T., TCHOU C., DUIKER H.-P., SAROKIN W., SAGAR M.: Acquiring the reflectance field of a human face. In *Proceedings of ACM SIGGRAPH 2000* (2000), pp. 145–156. 2

[DLG21] DESCHAINTRE V., LIN Y., GHOSH A.: Deep polarization imaging for 3d shape and SVBRDF acquisition. In *IEEE Conference on Computer Vision and Pattern Recognition, CVPR 2021, virtual, June 19-25, 2021* (2021), pp. 15567–15576. 2

[FCMB09] FRANCKEN Y., CUYPERS T., MERTENS T., BEKAERT P.: Gloss and normal map acquisition of mesostructures using gray codes. In *Proceedings of the 5th International Symposium on Advances in Visual Computing: Part II* (Berlin, Heidelberg, 2009), ISVC '09, Springer-Verlag, pp. 788–798. 1, 2

[GCP*09] GHOSH A., CHEN T., PEERS P., WILSON C. A., DEBEVEC P.: Estimating specular roughness and anisotropy from second order spherical gradient illumination. *Computer Graphics Forum 28*, 4 (2009). 1, 2, 5, 6

[GCP*10] GHOSH A., CHEN T., PEERS P., WILSON C. A., DEBEVEC P.: Circularly polarized spherical illumination reflectometry. *ACM Transactions on Graphics 29*, 6 (2010), 8. 2, 3

[GFT*11] GHOSH A., FYFFE G., TUNWATTANAPONG B., BUSCH J., YU X., DEBEVEC P.: Multiview Face Capture using Polarized Spherical Gradient Illumination. *ACM Transactions on Graphics 30*, 6 (2011), 1–10. 2

[GGG*16] GUARNERA D., GUARNERA G. C., GHOSH A., DENK C., GLENCROSS M.: BRDF representation and acquisition. *Computer Graphics Forum 35*, 2 (2016), 625–650. 2

[GTHD03] GARDNER A., TCHOU C., HAWKINS T., DEBEVEC P.: Linear light source reflectometry. *ACM Trans. Graph. (Proc. SIGGRAPH) 22*, 3 (2003), 749–758. 2

[MHP*07] MA W.-C., HAWKINS T., PEERS P., CHABERT C.-F., WEISS M., DEBEVEC P.: Rapid acquisition of specular and diffuse normal maps from polarized spherical gradient illumination. In *Rendering Techniques* (2007), pp. 183–194. 2

[MTHI03] MIYAZAKI D., TAN R. T., HARA K., IKEUCHI K.: Polarization-based inverse rendering from a single view. In *ICCV* (2003), pp. 982–987. 2

[Mül95] MÜLLER V.: Polarization-based separation of diffuse and specular surface-reflection. In *Mustererkennung 1995*. Springer, 1995, pp. 202–209. 2

[NDVZJ19] NIMIER-DAVID M., VICINI D., ZELTNER T., JAKOB W.: Mitsuba 2: A retargetable forward and inverse renderer. *ACM Transactions on Graphics 38*, 6 (11 2019). 3

[NFB97] NAYAR S. K., FANG X.-S., BOULT T.: Separation of reflection components using color and polarization. *IJCV 21*, 3 (1997). 2

[RPG16] RIVIERE J., PEERS P., GHOSH A.: Mobile Surface Reflectometry. In *Computer Graphics Forum* (2016), vol. 35. 2

[RRFG17] RIVIERE J., RESHETOUSKI I., FILIPI L., GHOSH A.: Polarization imaging reflectometry in the wild. *ACM Transactions on Graphics 36*, 6 (2017). 1, 2, 3, 4, 5

[RWS*11] REN P., WANG J., SNYDER J., TONG X., GUO B.: Pocket reflectometry. *ACM Trans. Graph. 30*, 4 (July 2011), 45:1–45:10. 2

[SSIK99] SAITO M., SATO Y., IKEUCHI K., KASHIWAGI H.: Measurement of surface orientations of transparent objects by use of polarization in highlight. *J. Opt. Soc. Am. A 16*, 9 (1999), 2286–2293. 2, 5

[TDG18] TOISOUL A., DHILLON D. S., GHOSH A.: Acquiring spatially varying appearance of printed holographic surfaces. *ACM Trans. Graph. 37*, 6 (dec 2018). 2

[TVC07] THILAK V., VOELZ D. G., CREUSERE C. D.: Polarization-based index of refraction and reflection angle estimation for remote sensing applications. *Appl. Opt. 46*, 30 (2007), 7527–7536. 2, 5

[WB91] WOLFF L. B., BOULT T. E.: Constraining Object Features Using a Polarization Reflectance Model. *IEEE Transactions on Pattern Analysis and Machine Intelligence 13*, 7 (1991), 635–657. 2

[WLL*09] WEYRICH T., LAWRENCE J., LENSCH H. P. A., RUSINKIEWICZ S., ZICKLER T.: Principles of appearance acquisition and representation. *Found. Trends. Comput. Graph. Vis. 4*, 2 (Feb. 2009), 75–191. 2

[WSM11] WANG C.-P., SNAVELY N., MARSCHNER S.: Estimating dual-scale properties of glossy surfaces from step-edge lighting. *ACM Trans. Graph. 30*, 6 (Dec. 2011), 172:1–172:12. 2